The isotropic and anisotropic interactions of the alternating ferromagnetic quasi-one-dimensional magnet $[Cu_4(ndpa)_2(H_2O)_6Cl_2]\cdot 4H_2O$

2003 J. Phys.: Condens. Matter 15 4477

(http://iopscience.iop.org/0953-8984/15/25/315)

INSTITUTE OF PHYSICS PUBLISHING JOURNAL OF PHYSICS: CONDENSED MATTER

J. Phys.: Condens. Matter **15** (2003) 4477–4486 PII: S0953-8984(03)59362-6

The isotropic and anisotropic interactions of the alternating ferromagnetic quasi-one-dimensional magnet $[Cu_4(ndpa)_2(H_2O)_6Cl_2]\cdot 4H_2O$

Yasid Boudam[1], Gerda Fischer[1], Jochen Hagel[1], Erik Herrling[1], Bernd Pilawa[1], Christopher E Anson[2], Muralee Murugesu[2] and Annie K Powell[2]

[1] Physikalisches Institut, Universität Karlsruhe (TH), Wolfgang-Gaede-Str. 1, 76128-Karlsruhe, Germany
[2] Institut für Anorganische Chemie der Universität Karlsruhe (TH), 76128-Karlsruhe, Germany

E-mail: bernd.pilawa@pi.uni-karlsruhe.de

Received 10 February 2003
Published 13 June 2003
Online at stacks.iop.org/JPhysCM/15/4477

Abstract

The magnetic properties of $[Cu_4(ndpa)_2(H_2O)_6Cl_2]\cdot 2H_2O$ are studied by static and dynamic magnetic susceptibility measurements. The static susceptibility measurements between 2 and 300 K reveal ferromagnetically coupled Cu(II) dimers ($J/k_B = +24.0 \pm 0.5$ K). Two further exchange constants $J'/k_B = -0.40 \pm 0.02$ K and $J''/k_B = 2.2 \pm 0.2$ K are determined by zero-field ac-susceptibility measurements in the temperature range between 12 and 0.4 K. The exchange couplings are assigned by means of electron spin resonance measurements which show that Cu_4:Cl realizes a ferromagnetic alternating spin-$\frac{1}{2}$ Heisenberg chain with an antiferromagnetic interchain coupling.

1. Introduction

The relation between structure and magnetic properties plays an important role in the understanding of the magnetism of molecular compounds [1–6]. The information is necessary for the design and preparation of molecular-based materials exhibiting specific magnetic properties such as magnetic chain systems [7, 8] or single-molecule magnets [9–11]. It is well known that the triatomic carboxylate bridge –O–C–O– leads to an effective exchange coupling of Cu(II) ions [12–15]. The carboxylate bridge offers a large variety of different bridging and coordination conformations which determine the strength and the ferro- or antiferromagnetic character of the exchange interaction. The coupling modes can be classified according to the site (*equatorial* or *apical*) where the oxygen atom coordinates the Cu(II) ion and by the relative orientation of the Cu(II) ion with respect to the carboxylate unit (*syn* or *anti*) [16]. The experimental information can be summarized by the following qualitative rules. An antiferromagnetic coupling can be expected when *equatorial* sites are bridged in the *syn–syn* or *anti–anti* mode, whereas the *syn–anti* mode can lead to a ferromagnetic coupling. On the

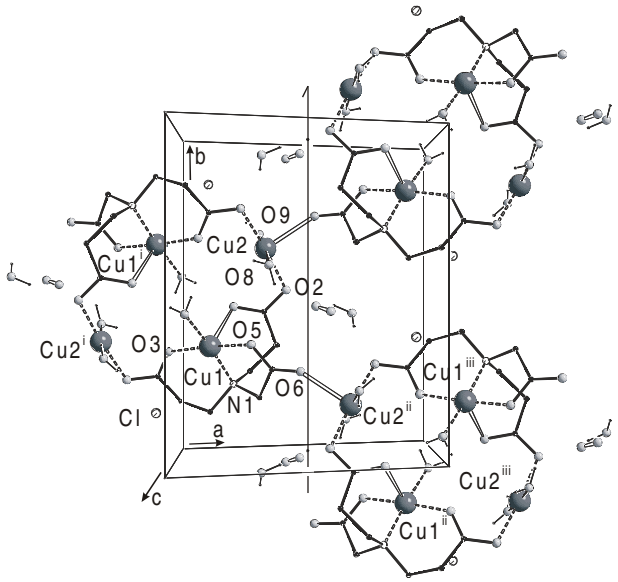

Figure 1. View of the unit cell of Cu_4:Cl (SCHAKAL).

other hand the *syn–anti* or *anti–anti/syn–syn* bridging mode of an *equatorial* and an *apical* site favours a small antiferromagnetic or ferromagnetic coupling, respectively [16–19].

In a recent work Murugesu *et al* [20] studied polynuclear Cu(II) complexes formed by the $ndpa^{3-}$ ligand (ndpa: nitrilo dipropionate acetate) and determined by magnetic measurements the exchange couplings via the various kinds of carboxylate bridges. In the case of $[Cu_4(ndpa)_2(H_2O)_6Cl_2]\cdot 2H_2O$ (Cu_4:Cl) a two-dimensional network of exchange coupled Cu(II) ions is found instead of magnetically isolated tetrameric Cu(II) units. The interesting magnetic properties of Cu_4:Cl are analysed in this paper. The structure of Cu_4:Cl is shown in figure 1 (space group $P2_1/c$, $a = 10.739$ Å, $b = 12.249$ Å, $c = 13.032$ Å, $\beta = 113.0°$). The two Cu(II) ions Cu(1) and Cu(1^i) are chelated by the $ndpa^{3-}$ ligand, and in turn are linked by the coordination of the outer carboxylate oxygens on the longer propionate arms of the ligands to two further $Cu(H_2O)_2$ units (Cu(2) and Cu(2^i)) resulting in a rhomboid array of four Cu(II) centres. The coordination of Cu(2) or Cu(2′) by one additional oxygen atom (O(6)) from the shorter acetate arm of an adjacent complex results in the formation of infinite sheets of linked tetranuclear units [20]. The tetranuclear units are characterized by an inversion centre and repeated by virtue of a two-fold screw axis (figure 1). There are three types of exchange couplings mediated by the intracluster *equatorial–equatorial syn–anti* (Cu(1)...Cu(2^i) and Cu(2)...Cu(1^i)), the *equatorial–apical syn–anti* (Cu(1)...Cu(2) and Cu(1^i)...Cu(2^i)) and the intercluster *equatorial–apical anti–anti* (Cu(1)...Cu(2^{ii})) carboxylate bridges. The magnetic properties of this Cu(II) network are studied by magnetic susceptibility and electron spin resonance measurements. It is shown that Cu_4:Cl realizes an alternating ferromagnetic spin-$\frac{1}{2}$ chain.

The plan of the paper is as follows. The results of the static and ac susceptibility are summarized in section 2. Measurements down to 2 K show an overall ferromagnetic coupling of the Cu(II) ions whereas the low-temperature measurements down to 0.4 K reveal a small antiferromagnetic coupling. The analysis of the susceptibility measurements yield three exchange constants $J/k_B = +24.0 \pm 0.5$ K, $J'/k_B = -0.40 \pm 0.02$ K and $J''/k_B = +2.2 \pm 0.2$ K. When the exchange constants are assigned in analogy to Cu_4:NO_3—a

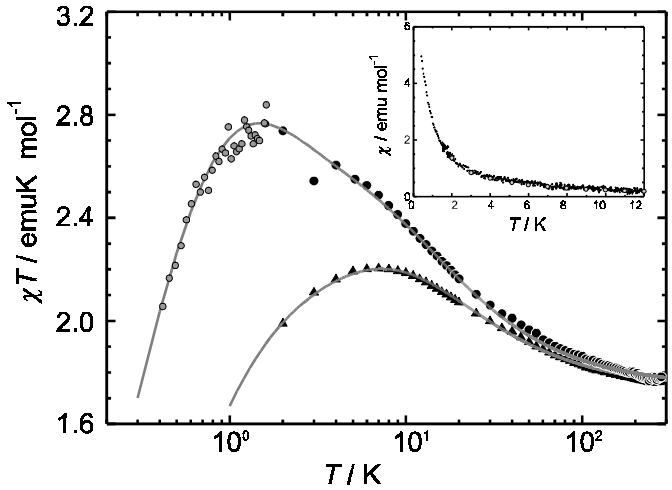

Figure 2. Magnetic susceptibility of Cu_4:Cl (black dots: static susceptibility, grey dots: ac susceptibility) and Cu_4:NO_3 (triangles). The calculated results (full curves) are explained in the text. Inset: comparison between the ac (small dots) and static susceptibility measurements (larger grey dots) of Cu_4:Cl.

related substance of magnetically isolated tetramers [20]—an alternating ferromagnetic chain structure results. The ESR results are discussed in section 3. These measurements confirm the assignment of the exchange constants and provide insight into the magnetic anisotropy of Cu_4:Cl.

2. Magnetic susceptibility

Figure 2 shows the susceptibility of polycrystalline samples of Cu_4:Cl. The static susceptibility is measured with a SQUID magnetometer (Quantum Design, Magnetic Properties Measurement System) for a magnetic field strength of 1 kOe in the temperature range between 2.0 and 300 K (sample mass 11.8 mg). The measurements of Cu_4:Cl are compared with those of Cu_4:NO_3 ($[Cu_4(ndpa)_2(H_2O)_8(NO_3)_2]\cdot 2H_2O$, sample mass 19.7 mg). Cu_4:NO_3 differs from Cu_4:Cl by two additional H_2O molecules which replace the coordination of Cu(2) or Cu(2′) by atom O(6) of the neighbouring cluster. This modification cuts the exchange path which exists between the tetranuclear units of Cu_4:Cl (for details see [20]). The magnetic susceptibility of the tetranuclear cluster Cu_4:NO_3 can be well approximated by the isotropic exchange Hamiltonian

$$H = -J(\vec{s}_1\vec{s}_2 + \vec{s}_3\vec{s}_4) - J'(\vec{s}_2\vec{s}_3 + \vec{s}_4\vec{s}_1). \tag{1}$$

The static magnetic susceptibility is calculated according to the formula [1]

$$\chi = N\frac{(\bar{g}\mu_B)^2}{3k_BT}\sum_{\{E_S\}} S(2S+1)(S+1)\exp(-E_S/k_BT)\Big/\sum_{\{E_S\}}(2S+1)\exp(-E_S/k_BT). \tag{2}$$

where the summation $\{E_S\}$ includes all the spin eigenstates of the Hamiltonian equation (1) which are $E_{S=0} = \frac{1}{2}(J+J') \pm \sqrt{J^2+J'^2-JJ'}$, $E_{S=1} = -\frac{1}{2}(J-J')$ and $\frac{1}{2}(J \pm J')$, $E_{S=2} = -\frac{1}{2}(J+J')$ [20]. $\bar{g}$ denotes the mean g factor of the Cu^{II} ions, N is the number of Cu_4 units and μ_B is the Bohr magneton. The parameters of Cu_4:NO_3 are $J/k_B = +24.0 \pm 0.5$ K, $J'/k_B = -0.80 \pm 0.05$ K with $g = 2.16$ from ESR measurements (see figure 2)[3], and agree

[3] In figure 7 of [20] the denotation of sample 2 and 4 in the figure caption are interchanged.

well with the results obtained in [20][4]. The ferromagnetic coupling J can be assigned to the *equatorial–equatorial syn–anti* carboxylate bridge between Cu(1) and Cu(2^i) whereas the small antiferromagnetic coupling is attributed to the *equatorial–apical syn–anti* carboxylate bridge between Cu(1) and Cu(2) [20].

The Hamiltonian equation (1) cannot be applied in the case of Cu_4:Cl since the tetranuclear units are magnetically coupled. The ESR measurements (see section 3) show that the intercluster exchange interaction is not negligible. At 2 K the magnetization of Cu_4:Cl follows the field dependence expected for spin 1. This indicates that the magnetic properties of Cu_4:Cl at 2 K are determined by the ferromagnetically coupled Cu(II) dimers. It can be concluded from the fact that $\chi T_{max} = 2.8$ emu K mol^{-1} is larger than $\chi T = 2.33$ emu K mol^{-1} ($\bar{g} = 2.16$)—expected for a system of free spins 1—that these dimers are ferromagnetically coupled. In [20], the analysis of the magnetic results on Cu_4:Cl was limited to an average value of the interdimer exchange interaction. The susceptibility measurements were extended to a lower temperature in order to obtain specific information about the interdimer exchange interaction and to establish the relation between the structural and magnetic properties.

The low-temperature range down to ∼0.4 K was studied by ac susceptibility measurements in a toploading ^{3}He cryostat (sample mass 0.59 mg). The induced ac signal was detected in a compensated pickup coil system with the usual lock-in technique. No static external magnetic field was applied during the measurements in order to avoid any saturation effect of the magnetization and the modulation field amplitude was below 2 Oe at a modulation frequency of ∼78 Hz. No out-of-phase ac signal was detected. This means, that the spin dynamics in the whole temperature range studied is so fast that the ac signal is simply proportional to the static magnetic susceptibility. The non-calibrated ac signal was adjusted to the static susceptibility measurements in the temperature range 2–12 K (see the inset of figure 2). These measurements reveal a small antiferromagnetic interaction, which was not expected according to the analysis presented in [20].

The antiferromagnetic coupling can originate either from a coupling within the two-dimensional Cu network or alternatively in an interaction of neighbouring Cu sheets. The second possibility is not likely, due to the small size of the dipolar interaction between two Cu(II) ions of neighbouring sheets (∼0.01 K). The effective interaction between two neighbouring sheets might be enhanced by short-range intraplane spin correlations. This effect is certainly small since the product χT is only slightly enhanced over the value expected for completely independent spin 1 units.

The magnetic properties of Cu_4:Cl are therefore analysed by a planar model where the spins are coupled according to the scheme shown in figure 3. According to the crystal structure (see figure 1) pairs of Cu(II) ions are ferromagnetically coupled by J (bold lines in figure 3). By an intracluster interaction J' they are coupled to tetranuclear units (thin lines in figure 3). These units are linked by the intercluster interaction J'' (dotted lines in figure 3).

Since the experimental results indicate no long range spin correlation it can be assumed that the coupling scheme of figure 3 leads to an appropriate description of the experimental results when the periodic boundary conditions $s_1 = s'_1, s_5 = s'_5, s_9 = s'_9, s_{13} = s'_{13}$ and $s_{14} = s'_{14}$ are used. The matrix elements of the exchange Hamiltonian corresponding to figure 3 were calculated with the tensor operator technique [21, 22][5].

[4] Our equation (2) leads to equation (5) in [20] apart from a factor of 2 in front of B, which is a typewriting mistake and should be replaced by 1 (cf, e.g., [19]); note also that the exchange constants $2J_1$ and $2J_2$ in the Hamiltonian equation (4) of [20] have to be replaced by J and J' of the present paper.

[5] The coupling of 16 spin-$\frac{1}{2}$ leads to 9 total spin states. The Heisenberg Hamiltonian splits up into matrices with the following dimensions: $S = 0$:1430, $S = 1$:3432, $S = 2$:3640, $S = 3$:2548, $S = 4$:1260, $S = 5$:440, $S = 6$:104, $S = 7$:15, $S = 8$:1.

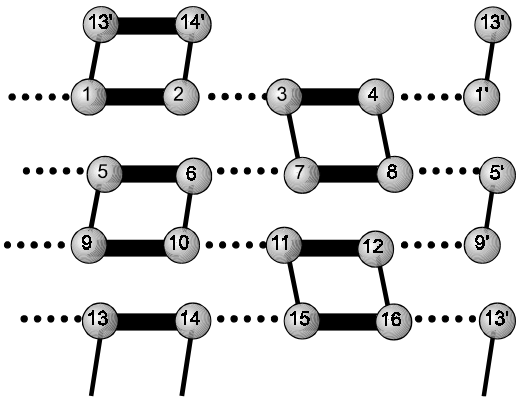

Figure 3. Coupling scheme of 16 spin-$\frac{1}{2}$ for the modelling of the magnetic properties of Cu_4:Cl. Bold lines: strong ferromagnetic intradimer coupling J, thin lines: intracluster coupling J', dotted lines: intercluster coupling J''.

The ferromagnetically coupled dimers $-J\vec{s}_{2n-1}\vec{s}_{2n}$, $(n = 1, 2, \ldots, 8)$ can be replaced by an effective spin 1 at temperatures below $\approx$4 K. Then the coupling scheme of figure 3 reduces with the above-mentioned periodic boundary conditions to the alternating spin 1 chain with the effective exchange constants $\tilde{J}' = \frac{1}{2}J'$ and $\tilde{J}'' = \frac{1}{2}J''$ as long $|J'|, |J''| \ll |J|$ holds. Due to the translation invariance of the alternating chain model it is no longer possible to differentiate between the inter- and intracluster exchange interaction. The fit of the experimental data with the coupling scheme of figure 3 (see figure 2) leads to the parameter $J'/k_B = +2.2 \pm 0.2$ K or -0.40 ± 0.02 K and $J''/k_B = -0.40 \pm 0.02$ or $+2.2 \pm 0.2$ K, respectively. In contrast to the results reported in [20], it reveals for the temperature variation of the susceptibility above $T \approx 100$ K that there exists no significant difference between Cu_4:Cl and Cu_4:NO_3 (figure 2). Therefore $J/k_B = +24$ K is fixed according to the results obtained for Cu_4:NO_3 and $\bar{g} = 2.16$ according to the ESR measurements (see section 3).

The intra- and intercluster exchange constants can be assigned in analogy to the related Cu_4:NO_3 cluster. For this cluster the *equatorial–apical syn–anti* carboxylate bridge between Cu(1)...Cu(2) and Cu(1^i)...Cu(2^i) leads to a small antiferromagnetic coupling of $J'/k_B = -0.8$ K. Therefore it is reasonable to assign the small antiferromagnetic coupling of $J'/k_B = -0.40 \pm 0.02$ K to the intracluster coupling between Cu(1)...Cu(2), Cu(1^i)...Cu(2^i) and the somewhat stronger ferromagnetic coupling to the *equatorial–apical anti–anti* carboxylate bridge between the tetranuclear units (e.g. Cu(1)...Cu(2^{ii}), compare figure 1). It will be shown in the following section that this assignment is supported by the analysis of the ESR measurements.

3. ESR measurements

3.1. Experimental results

ESR measurements were carried out in order to gain insight into the magnetism of the copper planes of Cu_4:Cl. The most important question concerns the intercluster exchange coupling via oxygen O(6).

Since the connected clusters are repeated by virtue of a two-fold screw axis along ***b*** (compare figure 1), the orientation of their g tensors is different which opens up the possibility to test the size of the intercluster exchange coupling. In the second part of this section the

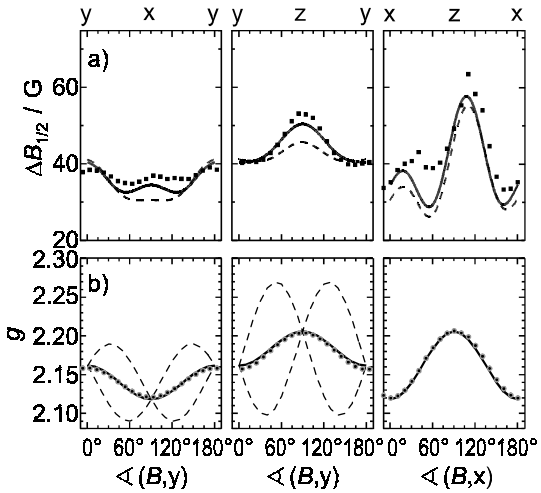

Figure 4. ESR results on Cu_4:Cl at room temperature. (a) Anisotropy of the linewidth $\Delta B_{1/2}$ (half-width at half-height) and (b) the g factor in three orthogonal planes. Dots: experimental results. Full and broken curves: calculations explained in the text.

anisotropic interactions of Cu_4:Cl are analysed and it is shown that the ESR linewidth shows features of low-dimensional spin diffusion caused by the two-dimensional nature of the copper network.

ESR was measured with a Bruker ESP300E X-band spectrometer (9.5 GHz) which was equipped with a rectangular cavity and an Oxford ESR900 cryostat. During the measurements the sample was covered by vacuum grease. The ESR signal could always be characterized by one Lorentzian absorption line. The studied crystals ($\sim 1 \times 1 \times 1$ mm^3) were oriented by means of a home-made goniometer and the measurements were carried out in the frame of reference fixed by the principal axis of the g tensor of Cu_4:Cl. The crystals could be oriented very accurately at room temperature and the results are shown in figure 4. The experimental g factors are $g_x = 2.121(1)$, $g_y = 2.157(1)$ and $g_z = 2.205(1)$. There is a small temperature dependence of the g factor and the linewidth.

3.2. General discussion of the ESR results

In order to estimate the orientation of the principal axis x, y, z of the g tensor of Cu_4:Cl within the unit cell the g tensor has to be modelled. The g tensor of Cu_4:Cl results from the average of the g tensor of copper atoms Cu(1), Cu(2) and the atoms Cu(1^{ii}) and Cu(2^{ii}) of the rotated unit (see figure 1). Within the Cu_4:Cl cluster the atoms Cu(1^{i}) and Cu(2^{i}) are related by inversion symmetry with Cu(1) and Cu(2) (the same holds for the pair Cu(1^{ii}), Cu(2^{ii}) and Cu(1^{iii}), Cu(2^{iii})) so that these ions are magnetically equivalent. The coordination environment of the copper ions is approximately square pyramidal with an elongated distance between the apical atom and the basal plane (see figure 1 and [20]). In order to restrict the number of free parameters it is assumed that the g tensor can be approximated by an axial tensor with $g_\parallel > g_\perp$ [23]. The basal plane of Cu(1) is defined by the atoms O(3), N(1) and O(5) and the basal plane of Cu(2) by the atoms O(8), O(2) and O(9) (see figure 1). It turns out that a fit of the experimental data with the two parameters $g_\parallel, g_\perp$ is not possible. The differences in the coordination environment of Cu(1) and Cu(2) suggest that their g tensors are also slightly different. The fit yields $g^{(1)}_{\perp/\parallel} = 2.10(2)/2.32(1)$ and $g^{(2)}_{\perp/\parallel} = 2.048(7)/2.35(2)$. Within this

model the x axis is nearly parallel to $\boldsymbol{c}\sphericalangle(\boldsymbol{x}, \boldsymbol{c}) = +4°$. The y axis is parallel to $\boldsymbol{b}$, according to the experimental results shown in figure 4. The real situation may slightly deviate from the model presented since the g tensors of the Cu ions are certainly not perfectly axial.

In general, without the exchange coupling of the Cu ions four different ESR signals could be expected corresponding to the four different g tensors of Cu(1), Cu(2) and the rotated pair $Cu(1^{ii})$, $Cu(2^{ii})$. The exchange coupling leads to one exchange narrowed ESR signal as long as the relative Zeeman energies of the Cu ions are small compared to the strength of their exchange interaction [24]. This is the case of the ferromagnetically coupled copper dimers $Cu(1)\ldots Cu(2^{i})$ and $Cu(2^{ii})\ldots Cu(1^{iii})$. The broken curves in figure 4(b) show the expected variation of the averaged g factor of these copper pairs. The full curves in figure 4(b) show the expected g factor of Cu_4:Cl. According to figure 4(b) the relative interdimer Zeeman energy $|(g^{(12)} - g^{(12)'})\mu_B B|/k_B$ in a magnetic field of 3.4 kOe is smaller than $\approx$0.05 K and consequently no linesplitting can be expected at 9.4 GHz. The energy difference increases with the strength of the magnetic field. Measurements at 95, 180 and 285 GHz were carried out at the ESR spectrometer of the high-magnetic field laboratory in Grenoble [25]. At these frequencies the anisotropic Zeeman interaction dominates and should lead to a linesplitting for an intercluster exchange coupling of $J''/k_B = -0.4$ K. A splitting could be observed for the related compound Cu_4:NO_3 but not for Cu_4:Cl. This result indicates that the ferromagnetic coupling of +2.2 K has to be assigned to the intercluster interaction J''.

3.3. Discussion of the ESR linewidth

The ESR linewidth is determined by the dipolar interaction, the anisotropic exchange interaction and the anisotropic Zeeman interaction. The anisotropic components of the Zeeman–Hamiltonian

$$H_{Zee}^{(ani)} = \sum_i (g_{zz}^{(i)} - \bar{g})\mu_B s_i^z B_0 + g_{xz}^{(i)}\mu_B s_i^x B_0 + g_{yz}^{(i)}\mu_B s_i^y B_0 \tag{3}$$

contribute to the ESR linewidth according to [24, 26, 27]

$$\Delta B_{1/2}^{(Zee)} = \gamma\left(\frac{B_0}{\bar{g}}\right)^2 \frac{1}{N}\sum_i (g_{zz}^{(i)} - \bar{g})^2 J_{Zee}(0) + \frac{1}{2}((g_{xz}^{(i)})^2 + (g_{yz}^{(i)})^2) J_{Zee}(\omega_0). \tag{4}$$

$\bar{g}$ denotes the mean value $\bar{g} = \frac{1}{4}(g_{zz}^{(\mathrm{Cu1})} + g_{zz}^{(\mathrm{Cu2})} + g_{zz}^{(\mathrm{Cu1}^{ii})} + g_{zz}^{(\mathrm{Cu2}^{ii})})$, $\gamma = \bar{g}\mu_B/\hbar$ and $\omega_0 = \gamma B_0$. The sum runs over all copper sites i. The spectral density related with the Zeeman interaction $J_{Zee}(\omega)$ is the Fourier transform of a two-spin correlation function [27]. Figure 5 shows the angular variation of $M_2^{(Zeeman)} = \gamma(\frac{B_0}{\bar{g}})^2 \frac{1}{N}\sum_i (g_{zz}^{(i)} - \bar{g})^2 + \frac{1}{2}((g_{xz}^{(i)})^2 + (g_{yz}^{(i)})^2)$. The anisotropy of $\Delta B_{1/2}$ is well reproduced in the xz plane. The variation in the xy and yz planes reflects essentially the difference $(g_{zz}^{(i)} - \bar{g})^2$ according to figure 4.

The dipolar broadening of the ESR line is given by the following formula [26, 28]:

$$\Delta B_{1/2} = \frac{9}{32}\hbar^2\gamma^3 \frac{1}{N}\sum_{i\neq j} (|F_{i,j}^{(0)}|^2 J(0) + 10|F_{i,j}^{(1)}|^2 J(\omega_0) + |F_{i,j}^{(2)}|^2 J(2\omega_0)). \tag{5}$$

With an isotropic g tensor the quantities in equation (5) are $F^{(0)} = (1 - 3\cos^2\theta)/r^3$, $F^{(1)} = \sin\theta\cos\theta e^{-i\varphi}/r^3$ and $F^{(2)} = \sin^2\theta e^{-i2\varphi}/r^3$ with the interdipole distance r and the angles θ, φ specifying the orientation of the magnetic field with respect to $\boldsymbol{r}$. The spectral density $J(\omega)$ is the Fourier transform of a four-spin correlation function which is normally frequency-independent for $\omega \ll |(J/\hbar)|$ [26]. Figure 5 shows the angular variation of $M_2^{(dipolar)} = \frac{9}{32}\hbar^2\gamma^3 \frac{1}{N}\sum_{i\neq j} (|F_{i,j}^{(0)}|^2 + 10|F_{i,j}^{(1)}|^2 + |F_{i,j}^{(2)}|^2)$ calculated with $g = 2$ (curve 1). When the anisotropy of the g tensor is included M_2 increases without changing the angular

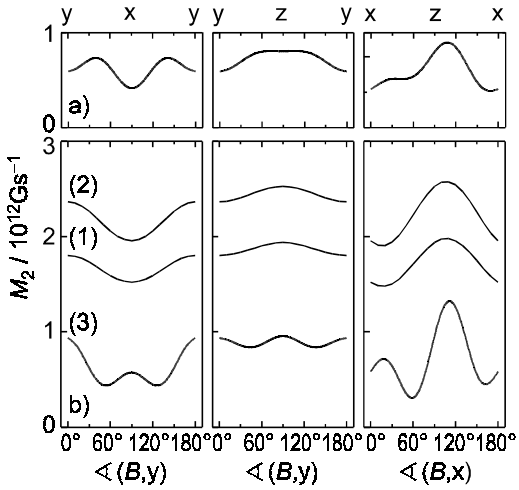

Figure 5. Expected anisotropy of the linewidth due to the anisotropic Zeeman interaction $M_2^{(Zeeman)}$ (a) and the dipolar interaction $M_2^{(dipolar)}$ (b): curve (1) calculated with an isotropic g factor $g = 2$, curve (2) calculated with an anisotropic g tensor (details see text) and curve (3) gives the $\omega = 0$ contribution to the linewidth.

variation significantly (curve 2, details are given in the appendix). Curve 3 shows the corresponding variation of $|F_{i,j}^{(0)}|^2$ which reproduces the essential features of the experimental results observed in the xz plane. This indicates that the secular contribution of $|F_{i,j}^{(0)}|^2$ should be enhanced. An enhanced spectral density $J(\omega = 0)$ is frequently found in low-dimensional systems due to the restriction of spin diffusion to one or two dimensions [29, 30]. These results confirm the conclusion in section 2 that the interplane interaction is negligibly small. The broken curve in figure 4(a) shows a fit of the dipolar contribution with the spectral densities $J(0)/3.5 = J(\omega_0) = J(2\omega_0) = 1.2 \times 10^{-11}$ s.

The description of the experimental results improves when the pseudo-dipolar anisotropic exchange interaction (PD exchange) is included. The PD exchange is added to the dipolar interaction of the ferromagnetically coupled Cu pairs of the tetranuclear clusters Cu(1)...Cu(2^i)/Cu(1^i)...Cu(2) and Cu(1^{ii})...Cu(2^{iii})/Cu(1^{iii})...Cu(2^{ii}) (cf the appendix). The PD tensor $A_{\mu,\mu'}$ is oriented as the averaged g tensor of the coupled ions $g^{(12)} = \frac{1}{2}(g^{(\mathrm{Cu1})} + g^{(\mathrm{Cu2})})$ and $g^{(12)'} = \frac{1}{2}(g^{(\mathrm{Cu1}^{ii})} + g^{(\mathrm{Cu2}^{ii})})$ [31] and the anisotropy $\eta = (A_x - A_y)/A_z$ is approximated by the anisotropy of the averaged g tensors, i.e. $(g_x^{(12)} - g_y^{(12)})/(g_z^{(12)} - \bar{g}^{(12)})$ (with $\bar{g}^{(12)} = (g_x^{(12)} + g_y^{(12)} + g_z^{(12)})/3$). The strength of the PD exchange is usually overestimated by the formula of Moriya [32] $(\Delta g/g)^2|J|$ for small values of J (Δg denotes the deviation of g from the free electron g factor). The spectroscopic work on the spin chains Cu-benzoate and *α-bis* (*N*-methylsalicylaldiminato)-Cu shows that the strength of the PD exchange and the dipolar interaction are comparable [33, 34]. The full curve in figure 4(a) is obtained when the contribution of the PD exchange with a strength of $A_z = -(g\mu_B)^2/r^3$ ($g = 2$ and $r = 4.466$ Å the distance between the Cu(1)–Cu(2^i) pair) and an anisotropy $\eta = -0.667$ resulting from the average of the g tensor $g^{(12)} = \frac{1}{2}(g^{(\mathrm{Cu1})} + g^{(\mathrm{Cu2})})$ is included. A quantitative analysis of the linewidth is not reasonable due to the large number of parameters but it is obvious that the anisotropy of $\Delta B_{1/2}$ can be understood in terms of the dipolar interaction and the PD exchange of the *equatorial–equatorial syn–anti* carboxylate bridge between Cu(1)...Cu(2^i) and Cu(2)...Cu(1^i).

When the temperature is lowered the g factor and the linewidth change slightly. This will not be discussed since it is difficult to discriminate precisely between the effects caused by the temperature and a possible misalignment of the crystal.

4. Conclusion

The magnetism of Cu_4:Cl is determined by the properties of three kinds of carboxylate bridges: the *equatorial- equatorial syn–anti* (1), the *equatorial–apical syn–anti* (2) and the *equatorial–apical anti–anti* (3). By a combined analysis of static and dynamic susceptibility measurements it was shown that bridge (1) leads to a ferromagnetic coupling $J/k_B = +24$ K, bridge (2) leads to a weak antiferromagnetic coupling $J'/k_B = -0.4$ K and bridge (3) to a weak ferromagnetic coupling $J''/k_B = +2.2$ K. Cu_4:Cl can be regarded as an alternating ferromagnetic spin chain with an non-negligible antiferromagnetic interchain coupling.

Acknowledgments

BP would like to thank A L Barra for her support during the high-field ESR measurements in Grenoble (project SO-4902). The work has been supported through the Human Potential Programme under contract no HPRI-1999-CT-00030 and by the Center for Functional Nanostructures (CFN) of the Deutsche Forschungsgemeinschaft (DFG) within project C3.4.

Appendix

The tensor of the dipolar interaction between spin i and j $H_{dipole} = D_{\mu,\mu'}(i,j)s_i^{\mu}s_j^{\mu'}$ is given by $D_{\mu\mu'}(i,j) = \frac{(g\mu_B)^2}{r_{ij}^3}(\delta_{\mu\mu'} - 3\hat{r}_{ij}^{\mu}\hat{r}_{ij}^{\mu'})$, if the g tensor is isotropic. If the anisotropy of the g tensor is included the tensor $D_{\mu\mu'}(i,j)$ becomes $D_{\mu\mu'}(i,j) = \frac{\mu_B^2}{r_{ij}^3}((\sum_{\nu=x,y,z} g_{\nu\mu}^{(i)}g_{\nu\mu'}^{(j)}) - 3(\sum_{\nu} g_{\nu\mu}^{(i)}\hat{r}_{ij}^{\nu})(\sum_{\nu} g_{\nu\mu'}^{(j)}\hat{r}_{ij}^{\nu}))$. $\vec{r}_{ij}$ denotes the connecting vector of the spins and $\hat{r}_{ij}$ the corresponding unit vector. From this tensor the trace $\frac{1}{3}\sum_{\mu=x,y,z} D_{\mu\mu}(i,j)$ is subtracted since it does not contribute to the anisotropy.

The pseudo-dipolar exchange is added to the dipolar interaction between a pair of spins according to $H = \sum_{\mu,\mu'=x,y,z}(D_{\mu,\mu'}(i,j) + A_{\mu,\mu'}(i,j))s_i^{\mu}s_j^{\mu'}$. The principal axes of the PD tensor $A_{\mu\mu'}(i,j)$ are determined by the principal axes of the averaged g tensor of the coupled ions $(g_{\mu\mu'}^{(i)} + g_{\mu\mu'}^{(j)})/2$ and differ therefore in general from those of $D_{\mu\mu'}(i,j)$.

The geometrical factors $F_{ij}^{(q)}$ are $F^{(0)} = \alpha_{zz}/(\bar{g}\mu_B)^2$, $F^{(\pm 1)} = -\frac{1}{3}(\alpha_{xz} \mp i\alpha_{yz})/(g\mu_B)^2$ and $F^{(\pm 2)} = -\frac{1}{3}(\alpha_{xx} - \alpha_{xx} \mp 2i\alpha_{xy})/(g\mu_B)^2$ with the abbreviation $\alpha_{\mu,\mu'} = D_{\mu,\mu'} + A_{\mu,\mu'}$.

References

[1] Kahn O 1986 *J. Magn. Magn. Mater.* **54–57** 1459
[2] Gatteschi D, Kahn O, Miller J S and Palacio F (ed) 1991 *Magnetic Molecular Materials (NATO ASI Series, No E198)* (Dordrecht: Kluwer–Academic)
[3] Dormann E, Winter H, Dyakonow W, Gotschy B, Lang A, Naarmann H and Walker N 1992 *Ber. Bunsenges. Phys. Chem.* **96** 922
[4] Kahn O 1993 *Molecular Magnetism* (Weinheim: VCH)
[5] Kahn O (ed) 1996 *Magnetism: A Supramolecular Function (NATO ASI Series, No C484)* (Dordrecht: Kluwer–Academic)
[6] Coronado E, Delhaes P, Gatteschi D and Miller J S (ed) 1996 *Molecular Magnetism: From the Molecular Assemblies to the Devices (NATO ASI Series, No E321)* (Dordrecht: Kluwer–Academic)

[7] Hatfield W E, Estes W E, Marsh W E, Pickens M W, ter Haar L W and Weller R R 1983 *Extended Linear Chain Compounds* vol 3, ed J S Miller (New York: Plenum) pp 43–142
[8] Landee C P 1987 *Organic and Inorganic Low-Dimensional Crystalline Materials (NATO ASI Series B)* vol 168, ed P Delhaes and M Drillon (New York: Plenum) pp 75–92
[9] Gatteschi D, Caneschi A, Pardi L and Sessoli R 1994 *Science* **265** 1055
[10] Stamp P C E 1996 *Nature* **383** 125
[11] Schwarzschild D 1997 *Phys. Today* **50/1** 17
[12] Bleaney B and Bowers K D 1952 *Proc. R. Soc.* A **214** 451
[13] Martin R L and Watermann R J 1957 *J. Chem. Soc.* 2545
[14] Lewis J, Mabbs F E, Royston L K and Smail W R 1969 *J. Chem. Soc.* A 291
[15] Costes P J, Dahan F and Laurent J P 1985 *Inorg. Chem.* **24** 1018
[16] Colacio E, Dominguez-Vera J M, Ghazi M, Kivekäs R, Klinga M and Moreno J M 1999 *Eur. J. Inorg. Chem.* 441
[17] Colacio E, Costes J P, Kivekas R, Laurent J P and Ruiz J 1990 *Inorg. Chem.* **29** 4240
[18] Colacio E, Dominguez-Vera J M, Moreno J M, Ruiz J, Kivekäs R and Romerosa A 1993 *Inorg. Chim. Acta* **212** 115
[19] Colacio E, Ghazi M, Kivekäs R and Moretno J M 2000 *Inorg. Chem.* **39** 2882
[20] Murugesu M, Clérac R, Pilawa B, Mandel A, Anson Ch E and Powell A K 2002 *Inorg. Chim. Acta* **337** 328
[21] Judd B R 1963 *Operator Techniques in Atomic Spectroscopy* (New York: McGraw-Hill)
[22] Gatteschi D and Pardi L 1993 *Gaz. Chim. Italiana* **123** 1
[23] Abragam A and Bleaney B 1970 *Electron Paramagnetic Resonance of Transition Ions* (Oxford: Clarendon)
[24] Bencini A and Gatteschi D 1990 *Electron Paramagnetic Resonance of Exchange Coupled Systems* (Berlin: Springer)
[25] Muller F, Hopkins M A, Coron N, Grynberg M, Brunel L C and Martinez G 1989 *Rev. Sci. Instrum.* **60** 3681
[26] Kubo R and Tomita K 1954 *J. Phys. Soc. Japan* **9** 888
[27] Pilawa B 1997 *J. Phys.: Condens. Matter* **9** 3779
[28] Abragam A 1961 *The Principles of Nuclear Magnetism* (Oxford: Clarendon)
[29] Boucher J P, Ahmed Bakheit M, Nechtschein M, Villa M, Bonera G and Borsa F 1976 *Phys. Rev.* B **13** 4098
[30] Benner H and Boucher J P 1990 *Physics and Chemistry of Materials with Low-Dimensional Structure* vol 9, ed L J De Jongh (Dordrecht: Kluwer–Academic) pp 323–378
[31] Banci L, Bencini A and Gatteschi D 1983 *J. Am. Chem. Soc.* **105** 761
[32] Moriya T 1960 *Phys. Rev.* **120** 91
[33] Herrling E 2001 *Thesis* Universität Karlsruhe (TH) (Göttingen: Cuvillier)
[34] Pilawa B, Herrling E and Odenwald I 2001 *J. Magn. Magn. Mater.* **226–230** 417